

Metallic bonding due to correlations: A quantum chemical ab-initio calculation of the cohesive energy of mercury

Beate Paulus¹ and Krzysztof Rosciszewski^{1,2}

¹ *Max-Planck-Institut für Physik komplexer Systeme, Nöthnitzer Straße 38, D-01187 Dresden, Germany*

² *Institute of Physics, Jagellonian University, Reymonta 4, PL 30-059 Krakow, Poland*

Solid mercury in the rhombohedral structure is unbound within the self-consistent field (Hartree-Fock) approximation. The metallic binding is entirely due to electronic correlations. We determine the cohesive energy of solid mercury within an ab-initio many-body expansion for the correlation part. Electronic correlations in the $5d$ shell contribute about half to the cohesive energy. Relativistic effects are found to be very important. Very good agreement with the experimental value is obtained.

Pacs-No.: 71.15.-m, 71.20.-b, 96.30.Dz

Mercury is a very special metal: It is a liquid at room temperature and it freezes at $T = 233\text{K}$ with a rhombohedral lattice ($a_0 = 3.005\text{\AA}$, $\alpha = 70.53^\circ$ [1]). The mercury dimer is a van der Waals bound molecule with a binding energy of about 0.05 eV [2], more than one magnitude lower than the bulk cohesive energy of 0.79 eV per atom [1]. Increasing the size of mercury clusters, the character of binding changes from van der Waals over covalent (around 20 atoms) to metallic (more than 100 atoms) [3].

The origin of the cohesion in the solid mercury metal is the topic of this letter. A mean-field Hartree-Fock treatment yields no binding: In contrast to the textbook knowledge of the metallic bond, the cohesion of mercury is entirely due to correlations. No surprise, the cohesive energy and the lattice constants of bulk mercury have been a long outstanding problem in computational physics [4–6]. Questions of particular interest are the influence of the d -shell correlation on the binding and the importance of relativistic effects. For the dimer, the d -shell correlation contributes with more than a factor of 2 to the dissociation energy [7,8]. Wavefunction-based methods with very large basis sets achieve good agreement with experiment. For the metallic solid, one could expect DFT calculations to give reasonable results, but different functionals yield quite different values of the cohesive energy [6]. As dimer or trimer can be handled with wavefunction-based methods, it seems natural to employ a many-body expansion for the cohesive properties of larger clusters or the solid. However, a straightforward many-body expansion with 2-body and 3-body forces taken from free clusters works properly for rare gas crystals [9] but fails for metallic mercury [6].

We propose a combined approach: The self-consistent field treatment is performed at the Hartree-Fock (HF)

level in the periodic 3-dimensional infinite solid [10] and the correlation energy is calculated within a many-body incremental scheme [11]. The latter embeds larger and larger fragments of the solid with shells of the same atoms and the same geometrical parameters, but describes them with a smaller basis. Thus the contribution of the metallic binding is calculated at a self-consistent field level in the infinite solid, while the correlation part, which is fairly local, is treated in finite embedded clusters with wavefunction based correlation methods.

The Hartree-Fock calculation is performed with the program package Crystal98 [10]. To deal with the scalar-relativistic effects, we apply a small-core scalar-relativistic pseudopotential [12] where the $5s^2p^6d^{10}6s^2$ electrons are treated explicitly. As basis set for Crystal98 we modify the valence-double-zeta (vdz, i.e. providing 2 atomic orbitals for each occupied crystal orbital) correlation-consistent basis set of Peterson [13] resulting in $(6s6p6d)/[4s4p3d]$. We frequently compare with results of a calculation with a non-relativistic small-core pseudopotential [12].

A first important observation is that mercury is not bound at the HF level (see Table II), both in the relativistic and the non-relativistic case. We checked that the system is unbound within the HF approximation for a wide range of lattice constants. Thus, the binding is entirely due to correlations. The cohesive energy at the HF level is less repulsive in the non-relativistic treatment. This is due to the smaller atomic sp splitting in the latter case. The p orbitals are too low in energy and their contribution to binding is overestimated.

The relativistic HF band structure (see Fig.1) and the density of states near the Fermi level are quite similar to the one obtained with LDA [5,14]. Between the L and Z points a conduction band crosses the Fermi level, responsible for the metallic behaviour. The logarithmic singularity which occurs with the HF approximation at the Fermi level is not discernible for the k -mesh used. The $5d$ bands are quite flat and placed well below the Fermi level. They overlap strongly with the $6s$ band at the Γ point, indicating the importance of the core-valence correlations. The strong sp mixing can be seen in the ℓ -decomposed density of states. Near the Fermi level, both have nearly the same magnitude. A Mulliken population analysis for the solid yields an electron transfer of 0.73 e from the s shell to the p shell, compared to 1.03 e in the nonrelativistic case. The non-relativistic HF band structure (dashed lines in Fig.1) shows a smaller sp -splitting at

Γ than the relativistic calculation. In a two-band model, one expects therefore the hybridization gaps, e.g., at the L or F point, to be larger and the p character of the valence band to be stronger, as it is seen in the bulk calculation (Fig.1).

We now proceed to the correlation treatment with the incremental scheme [11]. The correlation energy of the solid is expanded in 1-body increments ϵ_i , 2-body increments $\Delta\epsilon_{ij}$ and so on:

$$E_{\text{corr}} = \sum_i \epsilon_i + \sum_{i < j} \Delta\epsilon_{ij} + \sum_{i < j < k} \Delta\epsilon_{ijk} + \dots \quad (1)$$

The sums include groups of occupied localised orbitals. Note that we expand only the correlation part, in contrast to Moyano et al. [6], whose many-body expansion involves the total energy. A second difference is that we perform our calculations in embedded clusters to mimic the confinement of the electrons in the solid; for comparison see [15].

The incremental scheme obtains the energy increments from finite clusters calculations. For solid mercury the clusters were generated as follows: The rhombohedral structure can be viewed as a central atom surrounded by atom shells of various size. The first shell contains 12 atoms, 6 of them at distance a_0 and 6 at $1.15a_0$. We select the atoms which we want to correlate and surround each of them with atoms of the first shell. If the atoms to be correlated are far away, we select for the embedding also all atoms found within a cylinder of radius $1.15a_0$ around the connection line. The embedding atoms are described with a large-core pseudopotential [16] and only with a s basis set ($4s$)/[$2s$] [16]. This small basis set prevents the electrons to move onto the surface of the cluster, but still mimics the Pauli repulsion of the neighbourhood sufficiently well. Performing a HF calculation of the cluster (the basis set for the small-core pseudopotential is [3s1p1d], i.e. without unoccupied p basis functions) and localising the occupied orbitals [17], yields well localised orbitals on the individual atoms, which can be separated in embedding orbitals and orbitals to be correlated. With this procedure, we can generate local van der Waals like orbitals of the solid structure.

The delocalization of true metallic orbitals is treated via the incremental scheme as follows: Any orbital group i contains now all localised orbitals of atom i . In the first step we enlarge the basis set of the atom to be correlated to a reasonable quality, recalculate the integrals and re-optimize only the orbitals of the atom to be correlated in a HF calculation while the orbitals of the embedding are kept frozen. This provides us with fairly local orbitals on the atom to be correlated. On top of this HF calculation, we perform a Coupled-Cluster calculation with Single and Double excitations and perturbative treatment of the Triples (CCSD(T)) [18]. All calculation of the finite clusters are performed with the program package MOLPRO2002 [19]. The correlation energy provides us the

1-body increment ϵ_i .

The cohesive part of the 1-body increment

$$\Delta\epsilon_i^{\text{coh}} = \epsilon_i - \epsilon_{\text{atom}}^{\text{corr}}. \quad (2)$$

is defined as the change of the correlation energy of the atom due to surrounding it with other atoms. The correlation energy of the free atom $\epsilon_{\text{atom}}^{\text{corr}}$ is calculated with the same basis set as used in the finite cluster (basis functions on the surrounding, too). We list the cohesive part of the 1-body increment for different orbitals correlated and different basis sets applied in the first part of Table I. Basis A utilizes on Peterson's vdz basis ($7s7p6d1f$)/[$7s6p5d1f$]. Basis B utilizes on Peterson's vtz exponents and corresponds to ($10s9p7p2f1g$)/[$8s7p6d2f1g$] and Basis C on the vqz exponents, i.e. ($12s12p9d3f2g1h$)/[$9s8p7d3f2g1h$]. All values of $\Delta\epsilon_i^{\text{coh}}$ are repulsive. The atom in the metallic solid has a smaller correlation energy than the free atom, because the cage effect increases the level spacing and therefore decreases the correlation energy. For a reasonable basis set, e.g. Basis B or Basis C, where the Hilbert space is large enough to polarise the closed $5d^{10}$ and the $5s^2p^6$ shell, the correlation of the $5d^{10}$ shell is the same in the free atom and in the atom in the solid, but the correlation of the underlying $5s^2p^6$ shell yields in the solid a repulsive contribution of about 0.8 mH.

Next, we consider the contributions from the 2-body increments. All pairs of atoms up to $3.0a_0$ are embedded separately and, again, HF calculations are performed to generate the localised orbitals. The embedding part is kept frozen, while the orbitals of the atoms to be correlated are reoptimized with a better basis set and then correlated at the CCSD(T) level. The correlation of the $5d^{10}6s^2$ shell yields the 2-body correlation energy ϵ_{ij} . Only the non-additive part

$$\Delta\epsilon_{ij} = \epsilon_{ij} - \epsilon_i - \epsilon_j. \quad (3)$$

is required for the correlation energy of the solid (Eq. 1). To minimize the error due to the embedding, the 1-body increment which is subtracted in Eq. (3) has been determined in the same cluster with the second atom described with the small basis set. We have performed the calculation of the 2-body increments with Basis B up to a distance of $3.0a_0$, where the increment is less than 10 μH . We fit the van der Waals formula to the region from $1.5a_0$ to $2.8a_0$. The value $C_6=297$ atomic units is comparable with data from the literature [8,20,21]. Now, we can estimate the cohesive energy contributions from far-away pairs. If we include explicitly increments from all pairs smaller than $2.52a_0$ and estimate the rest (see Table II), the latter contribute only about 2% to the 2-body cohesive energy.

Table I lists the nearest-neighbour 2-body increment for different basis sets and different orbitals to be correlated. Pure valence correlations contribute about 40% (Basis B)

to the two-body increment, the $5d^{10}$ shell correlations are splitted in the $5d^{10}$ -valence (38%) and $5d^{10}$ - $5d^{10}$ (22%) correlation (Basis B). The correlation of the $5s^2p^6$ shell increases the magnitude of the 2-body increment by 6%. The increase of the 2-body increment applying Basis C instead of Basis B is about 7%. But probably still the basis set limit is not reached. The dissociation energy of the free Hg dimer obtained with an augmented vqz basis set, which is comparable to our Basis C for the solid, is still 13% below the estimated basis set limit [13].

The next step of the many-body expansion are the 3-body increments. It is well known that 3- and higher-body contributions are important for the binding in mercury [6]. We calculate all 3-body increments where two distances are $\leq 1.65a_0$ and the third $\leq 3.30a_0$. The 3-body increment

$$\Delta\epsilon_{ijk} = \epsilon_{ijk} - (\Delta\epsilon_{ij} + \Delta\epsilon_{ik} + \Delta\epsilon_{jk}) - (\epsilon_i + \epsilon_j + \epsilon_k) \quad (4)$$

is only the non-additive part due to the simultaneous correlation ($5d^{10}6s^2$ shell) of three atoms in the solid, and therefore expected to be small in comparison with the 2-body increment. The corresponding 2- and 1-body increments are calculated in the same embedding as the 3-body correlation energy ϵ_{ijk} . We apply Basis B for the 3-body increments. Summing all 3-body increments where two distances are $\leq 1.15a_0$ yields an attractive contribution to the cohesive energy of 5.1 mH, whereas the rest yields only 2.4 mH. If we follow Axilrod and Teller [22] and fit a dipole-dipole-dipole interaction to the 3-body increments where no distance is shorter than $1.5a_0$ and estimate the far away triangles with this fitting formula, the sum over the far-away triangles contributes less than 0.01 mH to the cohesion. This is due to the rapid decay of r^{-9} and a substantial cancellation of contributions from triangles with different angles. The basis set dependence of the 3-body increments was tested for the largest individual 3-body increment. Applying Basis C instead of Basis B yields an increase of 20%.

The 4-body contributions are calculated according to the scheme described for the 3-body increments. Here Basis A is applied. For one geometry Basis B is used, the increase of the increment is about 20%. Five connected 4-body clusters have been selected. The largest contribution comes from the linear one. Like for the linear 3-body increment, the presence of a highly polarisable central atom yields a significant increase of the correlation energy. But even for the large linear increments, the magnitude of the 4-body increment is by a factor of 4 smaller than the corresponding 3-body increment. In addition, most 4-body increments are repulsive, so we can expect an alternating sign series for the correlation energy of the solid.

Besides the contributions discussed up to now there are two small contributions to the cohesive energy resulting from the spin-orbit coupling and the zero-point energy. For the former, published values [7,8] for the dissociation

energy of the Hg dimer show only a small influence. The spin-orbit coupling of the $5d$ shell should be not so much different in the solid and the free atom, therefore the net effect on the cohesive energy should be small.

The latter one is due to zero-point phonon degrees of freedom. An estimation of the zero-point energy can be done with the Debye model $E_{\text{ZPE}} = \frac{9}{8}k_B\Theta_D$ [23], with the Debye temperature $\Theta_D=71.9\text{K}$ for mercury [24].

We have summarized our results in Table II. The HF part of the cohesive energy is repulsive, the 1-body correlation contribution to the cohesive energy is repulsive, too. The main contribution to the binding comes from the 2-body increments, with about half of this originating from the core-valence correlation of the d shell. Without correlating the d shell solid mercury would not be bound. The non-relativistic 2-body increments yield a significant over-binding. The 3-body contributions of the valence shell are attractive, whereas the 3-body contributions of the d shell are repulsive, reducing the 3-body contributions to about 10% of the 2-body contributions. Furthermore, the non-relativistic 3-body terms are strongly over-binding. This is due to the enlarged valence correlations and to the fact that the non-relativistic d shell is not interacting with the s -band at the Γ point (see Fig.1). Both lead to a too small repulsive part due to the core-valence correlation. The spin-orbit contribution and the zero-point energy can be neglected. If we extrapolate the 2-body-contributions to Basis C and to the inclusion of $5s^2p^6$ correlation we reach 74% of the experimental cohesive energy. If we further estimate the basis set error to the basis set limit from the dimer data, very good agreement with experiment (99%) is obtained.

In summary, we have presented a method, which allows us to determine the cohesive energy of solid mercury within the same accuracy with the experimental value as it was achieved for the much simpler rare gas crystals [9]. It can be easily systematically improved by expanding to higher orders and by applying better basis sets when the computing capabilities improve. Of course, the combination of extended HF calculations and the incremental scheme for the correlations can be applied to other metallic systems, too. But the specific nature of the mercury-mercury bond constitutes arguably the most interesting case.

Acknowledgement: The authors would like to thank Hermann Stoll (Stuttgart, Germany), Peter Fulde (Dresden, Germany) and Erich Runge (Dresden, Germany) for many valuable discussions and Peter Schwerdtfeger (Auckland, New Zealand), who first drew their attention to the mercury puzzle.

- [1] CRC Handbook of Chemistry and Physics, CRC Press, New York (1997).
- [2] A. Zehnacker, M.C. Duval, C. Jouvét, C. Lardeux-Dedonder, D. Solgadi, B. Soep, O. Benoist d'Azy, J. Chem. Phys. **86**, 6565 (1987).
- [3] H. Haberland, H. Kornmeier, H. Langosch, M. Oschwald and G. Tanner, J. Chem. Soc. Faraday Trans. **86**, 2473 (1990).
- [4] P.P. Singh, Phys. Rev. Lett. **72**, 2446 (1994).
- [5] P.P. Singh, Phys. Rev. **B 49**, 4954 (1994).
- [6] G.E. Moyano, R. Wesendrup, T. Söhnel and P. Schwerdtfeger, Phys. Rev. Lett. **89**, 103401 (2002).
- [7] M. Dolg and H.-J. Flad, J. Phys. Chem. **100**, 6147 (1996).
- [8] P. Schwerdtfeger, R. Wesendrup, G. Moyano, A. Sadlej, J. Greif, F. Hensel, J. Chem. Phys. **115**, 7401 (2001).
- [9] K. Rosciszewski, B. Paulus, P. Fulde and H. Stoll, Phys. Rev. **B 60**, 7905 (1999).
- [10] V.R. Saunders, R. Dovesi, C. Roetti, et. al. *Crystal 98 User's Manual, Theoretical Chemistry Group, University of Torino* (1998).
- [11] H. Stoll, Phys. Rev. B **46** (1992) 6700.
- [12] D. Andrae, U. Haeussermann, M. Dolg, H. Stoll, and H. Preuss, Theor. Chim. Acta **77**, 123 (1990). (The corresponding non-relativistic pseudopotential is unpublished. The f and g projectors are omitted in the Crystal code.)
- [13] K.A. Peterson: *Recent Advances in Electron Correlation Methodology, Correlation consistent basis sets with relativistic effective core potentials. The transition metal elements Y and Hg*, edited by A.K. Wilson and K.A. Peterson (ACS, to be published).
- [14] S. Deng, A. Simon, and J. Köhler, Angew. Chem. Int. Ed. **37**, 640 (1998).
- [15] K. Rosciszewski, et al., in preparation
- [16] W. Küchle, M. Dolg, H. Stoll, and H. Preuss, Mol. Phys. **74**, 1245 (1991).
- [17] J. M. Foster and S. F. Boys, Rev. Mod. Phys. **32** (1960) 296.
- [18] C. Hampel, K. Peterson and H.-J. Werner, J. chem. Phys. **99**, 5219 (1993).
- [19] MOLPRO version 2002.6 - a package of *ab-initio* programs written by H.-J. Werner and P. J. Knowles with contributions from J. Almlöf, et. al.
- [20] B. Hartke, H.-J. Flad and M. Dolg, Phys. Chem. Chem. Phys. **3**, 5121 (2001).
- [21] C. F. Kunz, C. Haettig, B. A. Hess, Mol. Phys. **89**, 139 (1996).
- [22] B. M. Axilrod and E. Teller, J. Chem. Phys. **11**, 299 (1943).
- [23] B. Farid and R. W. Godby, Phys. Rev. B **43**, 14248 (1991).
- [24] C. Kittel, *Introduction to Solid State Physics*, 7. ed, Wiley, New York (1996).

	Basis	$6s^2$	$5d^{10}6s^2$	$5s^25p^65d^{10}6s^2$
$\Delta\epsilon_1^{\text{coh}}$	A	+0.004287	+0.004740	+0.005390
	B	+0.004230	+0.004260	+0.005089
	C	+0.004168	+0.004210	+0.0049801
$\Delta\epsilon_{12}$	A	-0.003468	-0.009648	-0.010291
	B	-0.004107	-0.009862	-0.010487
	C	-0.004278	-0.010550	-0.011268

TABLE I. The correlation contribution to the cohesive energy of the 1-body increment $\Delta\epsilon_1^{\text{coh}}$ and the nearest-neighbour 2-body increment $\Delta\epsilon_{12}$ (both in Hartree) are listed above for different basis sets (detailed description in the text) and different orbitals to be correlated.

	$6s^2$ rel.	$5d^{10}6s^2$ rel.	$5d^{10}6s^2$ non-rel.
Hartree-Fock	+36.2	+36.2	+17.4
$\Delta\epsilon_i^{\text{coh}}$	+4.2	+4.3	+3.9
2-body up to $2.52a_0$	-25.0	-50.0	-62.0
far away 2-body		-1.1	
ext. to Basis C and $5s^2p^6$ corr.		-6.6	
3-body in the first shell	-10.3	-5.1	-15.7
3-body in the second shell		-2.4	
est. for far away 3-body		≤ -0.1	
4-body (selected clusters)		+3.0	
spin-orbit		≤ -0.1	
zero-point energy		+0.3	
calc. cohesive energy		-21.4	
est. to basis limit (from dimer)		-7.5	
exp. cohesive energy		-29.0	

TABLE II. The different contributions to the cohesive energy of mercury in mHartree per unit cell.

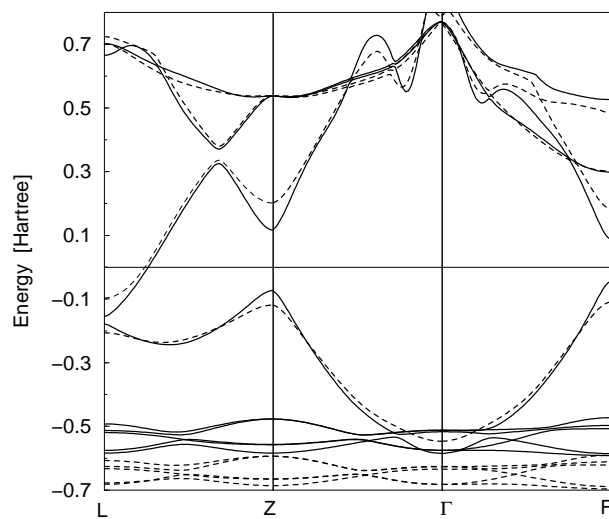


FIG. 1. The Hartree-Fock band structure of mercury at the experimental lattice constant of the rhombohedral structure. The Fermi energy is set to zero separately for the relativistic (full line) and for the non-relativistic calculations (dashed line).